Investigation of the Surface Produced by Shape Adaptive Polishing

Muhammad Mubashar Saeed

Department of Mechanical Engineering, Nanjing University of Science and Technology, Nanjing, China

Email address:

engr_mubasharsaeed@yahoo.com

Abstract: Ultra-precision machining (UPM), is renowned for manufacturing products with high precision and surface quality has found diverse application in the optics, automobile, medical instruments, and aerospace industries. Shape adaptive bonnet polishing (SABP), which uses a flexible, non-rigid bonnet tool can be used an alternative ultra-precision polishing method for polishing of complex and delicate microstructures. This paper aims at the investigation on the surface roughness produced by SABP by experimental and analytical model as well as scrutinizing the effects of polishing time and tool offset on tool imprints and surface roughness within the SABP process. Notably, our analytical model highlights the significant influence of polishing time over offset distance for enhancing surface quality, due to its capacity to generate a tool influence curve with a high radius of curvature. The elongation of polishing time leads to a deeper and more flattened tool influence curve, thus resulting in an improved surface quality, a conclusion further affirmed by our experimental outcomes. The utilization of SABP has demonstrated a capacity to enhance workpiece surface quality tenfold, yielding a smooth and uniformly polished surface with surface roughness of 0.008μm. In light of these results, to enhance surface quality further, the study advocates for the prioritization of extending polishing time over altering tool offset in ultra-precision machining.

Keywords: Polishing, Ultra-Precision Polishing, Bonnet Polishing, Shape Adaptive Bonnet Polishing

1. Introduction

With the development of manufacturing, ultra-precision machining has become a significant research area. Ultra-precision machining involves the manufacturing of products with a very high precision level, till atomic scale (0.2-0.4 nm), and surface quality, less than 10 nm [1, 4]. It is utilized in several applications such as automobile industry, medical instruments, aerospace industry, defense industry, communication industry, high-resolution camera lens manufacturing, etc. It has a great footprint in the revolution of optics industry [5].

Ultra-precision polishing is one of the ultra-precision machining processes which involves using a polishing tool in combination with a precise polishing action to remove a small amount of material from surface of the workpiece. It aims to reduce residual surface topography, sub-surface layer, and previous process defects, and improve the surface quality, producing a smooth, precise, and clean surface, meeting the quality requirements [6, 8]. It is applied as the last process in the manufacturing process after diamond turning or grinding. Ultra-precision polishing has the capability to create ultra-precise freeform surfaces with sub-micrometric form accuracy and nanometric surface roughness. There are different types of ultra-precision polishing processes such as small tool polishing (STP) [9], magnetorheological finishing (MRF) [10], bonnet polishing [11, 12], stressed-lap polishing (SLP) [13], fluid jet polishing (FJP) [14], and ion beam polishing (IBP) [15]. The main disadvantages of these ultra-precision polishing processes methods are tool wear, sub-surface damage, edge effects, mid spatial frequency errors, high equipment cost, low polishing efficiency, and unstable removal function, etc.

2. Shape Adaptive Bonnet Polishing

Shape adaptive bonnet polishing (SABP) is a special type of ultra-precision polishing, which involves the use of a flexible non rigid bonnet tool to polish complicated and delicate

microstructures in addition to difficult-to-cut materials [16]. This tool can adapt to the surface being polished, and abrasive particles are embedded into the external pad to remove material from the surface, achieving the desired finish [12, 17]. The SABP tool, is composed of several layers of different materials. A spherical rubber membrane reinforced with a Kevlar fabric serves as the inner layer to adapt the workpiece surface [17]. In order to reduce the tool distortion due to the applied inner air pressure, the Kevlar layer is inserted between two rubber layers. In order to obtain a precise centre and accurate shape of the sphere, the rubber tool is dressed on machine with a coarse grinding wheel. A second deformable layer, made up of intertwined textile and metal fabric, is applied to the tool surface, where hard pellets, with diamond abrasives embedded inside, are deposited on the cloth. The applied force can be controlled by the applied air pressure, while the spot area is controlled by the geometrical position of the tool with respect to the workpiece shape [17]. In order to control the contact spot shape and tool setting, Wang et al. proposed embedding a thin metal sheet of aluminium, stainless steel, or copper shaped to fit the inner surface into the rubber membrane. Stainless steel has been proved that it can provide the largest contact pressure [18].

Beaucamp et al. presented a paper involving the study of shape adaptive grinding (SAG) mechanism, which involves in SABP [19]. According to the tool radius and inclination angle, and workpiece shape, the grinding area is determined. The applied force on the grinding area controls the depth of penetration of the grinding grains. They considered in their study the size and shape of abrasive pellets, their overtime evolution, along with other parameters such as grinding forces, and modes associated with energy and chip thickness. Beaucamp et al. developed this study by considering the brittle ductile transition in the application of ceramics machining [20]. S. Bode et al. presented a study including single grain steel grit grinding in ploughing mechanism against an aluminum workpiece [21]. They included the latest empirical relation to predict material damage and failure namely Johnson Cook damage model. Kareer et al. built their study based on multi nano tests, for example nano scratches and nano indentations, has been performed and presented for berkovich tip on a single Copper crystal compared with lattice rotation field deformations and distortions [22]. A. Alaboodi and Z. Hussain built a finite element model of nano indentation testing of various thin film coatings [23]. They modelled various shapes and types of indenters using finite element analysis (FEA) using thin film characterizations. For the investigation of surface roughness experimentally, Cao et al. compared the SAG methods and validated the results [24]. Lee et al. carried out an interesting FEA tribological study using Abaqus software the new module XFE with experimental validations [25]. In their analysis, the effects of changing scratch tip size and coefficient of friction have been observed. In the numerical model only values were changed, while in the experimental study, material has been changed as well. Conical, semi-circular, berkovich, and Vickers indenter shapes have been used in symmetric conditions with drucker prager model being used for material.

Zhang et al. [26] in addition to J. Zhang and H. Wang [27] proved that the tool influence function (TIF) of SABP can be represented as a Gaussian-like curve and it depends on workpiece and grits geometrical, physical, mechanical, and chemical properties. It determines the workpiece surface profile and quality. Wang et al. succeeded to model the TIF using finite element analysis (FEA) and validated it experimentally [28]. Ke et al. proved, using FEA, that the M-shaped curve is more suitable for polishing using large tool offset [29].

This paper gives an experimental investigation into the effect of polishing time and tool offset on tool imprints and the produced surface roughness in SABP. In addition, the tool imprints have been modelled analytical.

3. Experimentation

The experiments have been conducted on customized CNC polishing machine, where the experimental setup is shown in Figure 1. The used shape adaptive tool was 8 mm*8 mm*3 mm as shown in Figure 2. It is supported by a customized spindle. The tool is moved along the raster scan step on a 1 mm × 1 mm of the workpiece. The workpiece material was brass which has several applications in industry which require high precision and surface quality. The workpiece was secured in a force sensor, which is fixed on the machine table, while the polishing head is moving to perform the polishing of the workpiece. There are two main experiments, Table 1, to investigate the effect of polishing time and tool offset. Experiment 1 has been carried out for 20 minutes, utilizing a contact force of 0.5 N and a step distance of 0.2 mm. Experiment 2 was conducted utilizing the same parameters of experiment 1, but with longer polishing time of 30 minutes and a larger step distance of 4 mm.
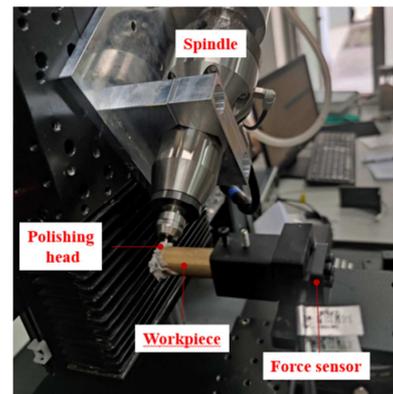

Figure 1. *The experimental setup of the polishing experiments.*


Figure 2. *The used shape adaptive tool.*

Table 1. Experiments Polishing Conditions.

| Experiment	Time [min]	Contact force [N]	Spindle speed [rpm]	Raster velocity [mm/min]	Step distance [mm]
Experiment 1	20	0.5	500	3	0.2
Experiment 2	30	0.5	500	3	0.4

The workpiece surface has been examined before and after polishing using ZYGO Nexview 3D optical profiler, the arithmetical mean height (Sa), root mean square height (Sq), and the maximum profile height (Sz) have been used as indices for roughness measurements.

4. Analytical Investigation of Tool Imprints in SABP

In order to show the effect of the polishing time, the tool influence curves for six paths for the two experiments have been modelled as shown in figures 3 and 4, based on J. Zhang and H. Wang's work [27]. Figure 3 shows the 3D tool imprints for the first experiment. However, the distance between two successive curves is small but the curves have smaller radius of curvature, producing rougher surface as compared to the second one. For the second experiments, however the doubled offset distance, the influence curve is deeper and is more flattened than that of the first experiments, producing smoother surface.
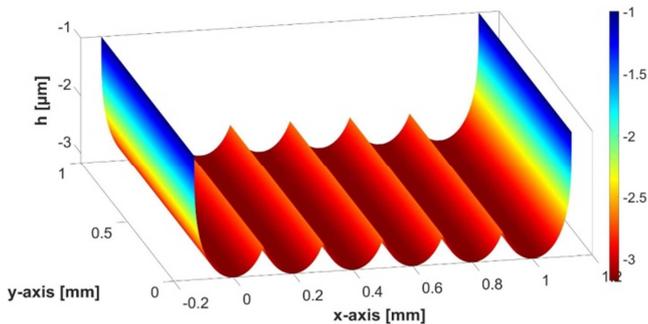
*Figure 3. A 3D Model for the Tool Imprints after Six Paths for the First Experiment.*
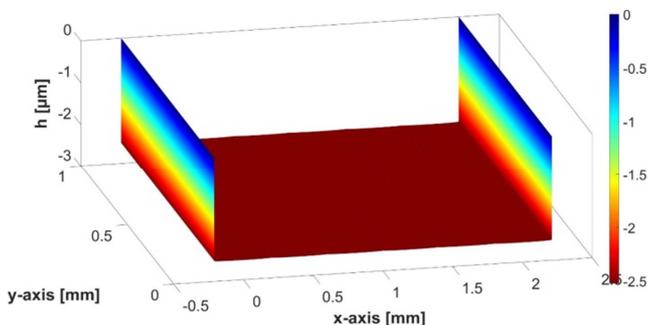
Figure 4. A 3D Model for the Tool Imprints after six Paths for the Second Experiment.

5. Results and Discussion

In this section, for both experiments, the produced surface from SABP will be investigated experimentally and analytically, in addition to the results of surface roughness measurements.

Figures 5-8 show the substantial effect of polishing in improving the surface quality for the two experiments by removing the machining marks. The figures 5-8 (a) show the workpiece surface before polishing due to the previous traditional machining process. The machining marks are obvious, and the fluctuations are large indicating low surface quality. The figures 5-8 (b) demonstrate the positive effect of SABP on the surface quality. The machining marks of the previous process have been eliminated producing a smooth surface with small surface fluctuations indicating good surface quality and uniform surface topography. The second experiment resulted in a better surface as quality and uniformity as the surface fluctuations are lower. This result can be explained with the effect of time in producing a deeper tool influence curve, however the larger offset distance as compared to the first experiment.
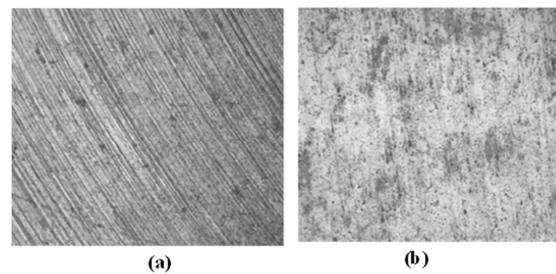
Figure 5. Optical Microscope Images of the Workpiece Surface for the first Experiment a) before Polishing and b) after 20 min. Polishing.
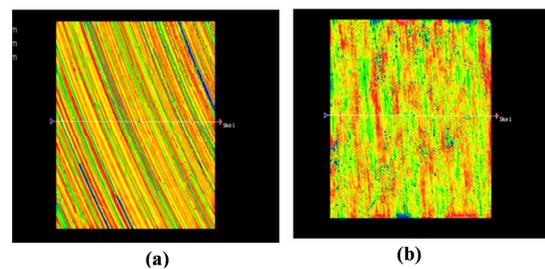

Figure 6. 3D Contour of the Workpiece Surface for the First Experiment a) Before Polishing and b) After 20 min. Polishing.
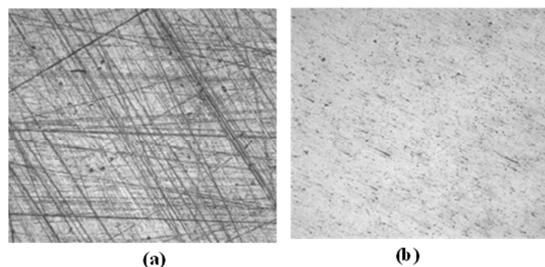
Figure 7. Optical Microscope Images of the Workpiece Surface for the Second Experiment a) before Polishing and b) after 30 min. Polishing.
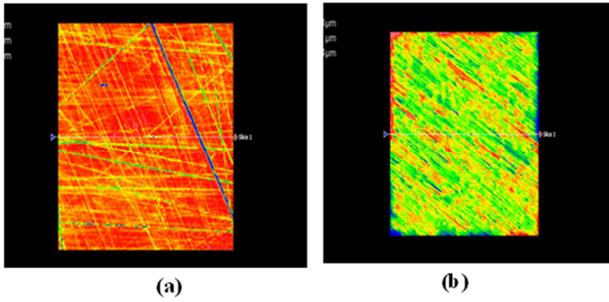
Figure 8. *3D Contour of the Workpiece Surface for the Second Experiment a) Before Polishing and b) After 30 min. Polishing.*

5.1. Tool Imprints Curve of SABP

The tool imprints of the first experiment for 1 and 4 mm^2 can be observed as real, 3D, and 2D images in figures 9-11. These results are consistent with that of the analytical model, section 3, with a small error of 13%. The polished surface is characterized by low variation indicating high repeatability of the process. Th effect of polishing is obvious in removing machining marks and producing smooth and uniform surface.
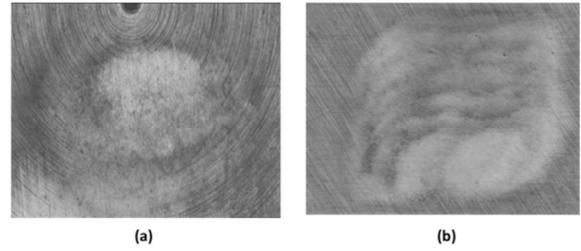
Figure 9. *Optical Microscope Images in a) 1 mm^2 Area and b) 4 mm^2 Area.*
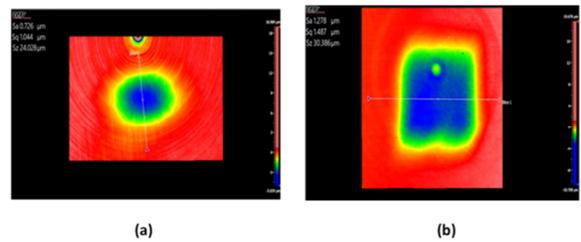
Figure 10. *3D Contour of the Workpiece Surface in a) 1 mm^2 Area and b) 4 mm^2 Area.*

(a)

(b)
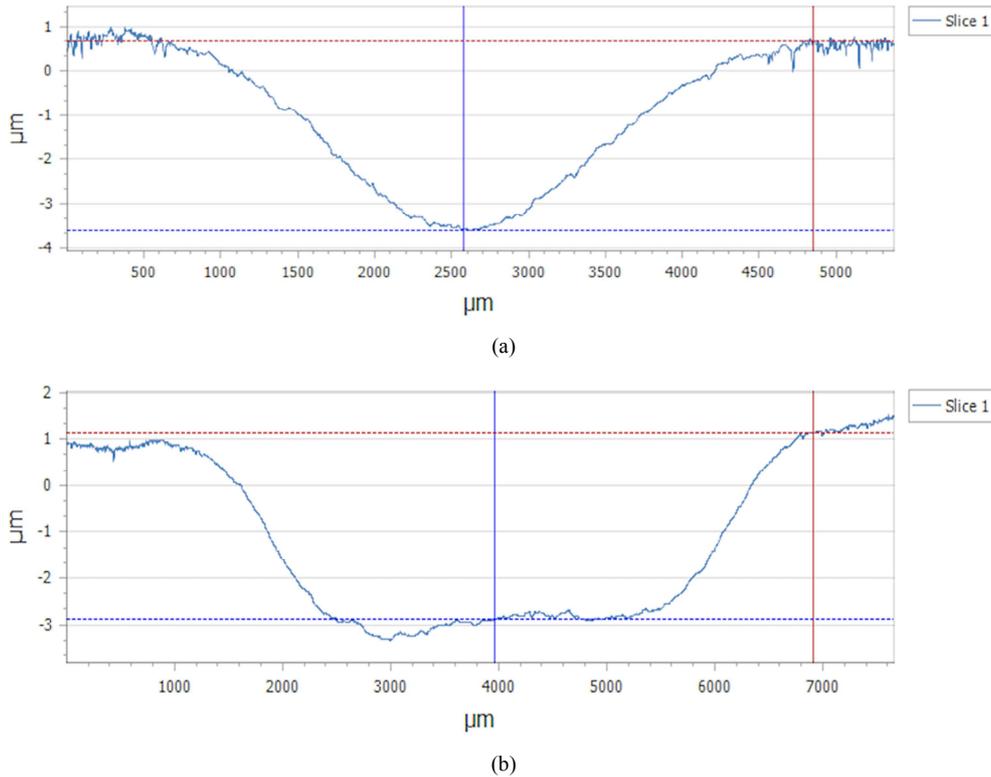
Figure 11. *2D Contour of the Workpiece Surface in a) 1 mm^2 Area and b) 4 mm^2 Area.*

5.2. Surface Roughness of the Produced from SABP

Figures 12 and 13 illustrates the workpiece surface profile before and after polishing for the first and the second experiments respectively. The profile of workpiece surface before polishing, for both experiments, the workpiece has 0.6μm maximum variation of the profile. The application of SABP reduced the surface roughness and profile variation by almost ten times. Table 2 shows the values of the surface roughness parameters before and after polishing for the two experiments. SABP resulted in a significant reduction of the surface roughness, R_a, of the workpiece from 0.097 μm to 0.012 μm by 88% surface roughness reduction for the first experiment and from 0.053 μm to 0.008 μm for the second one by 85% surface roughness reduction. However, the difference between reduction ratios is small, but the second experiment gives final better surface roughness. This can be explained by the effect of the tool imprints as explained in section 03. Although, doubling

step distance has a negative effect on the surface quality, but due to the effect of increasing polishing time on the influence curve, the quality has been enhanced. Hence, polishing time is more significant on surface quality than tool offset.
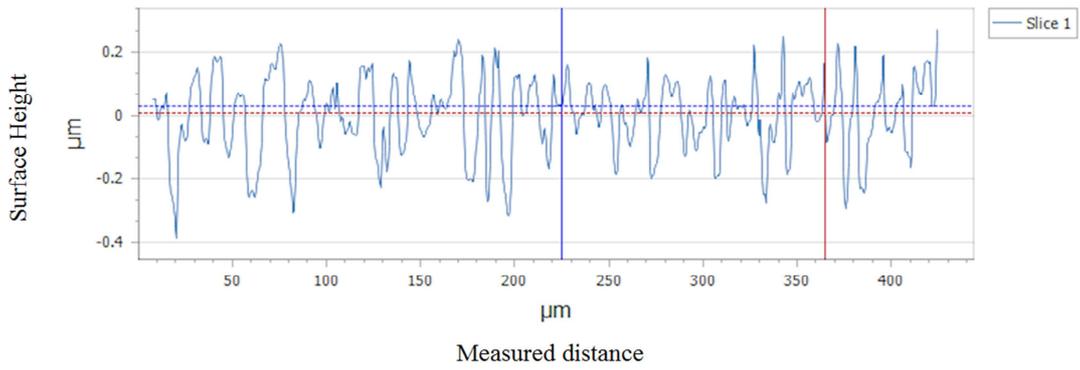
(a)
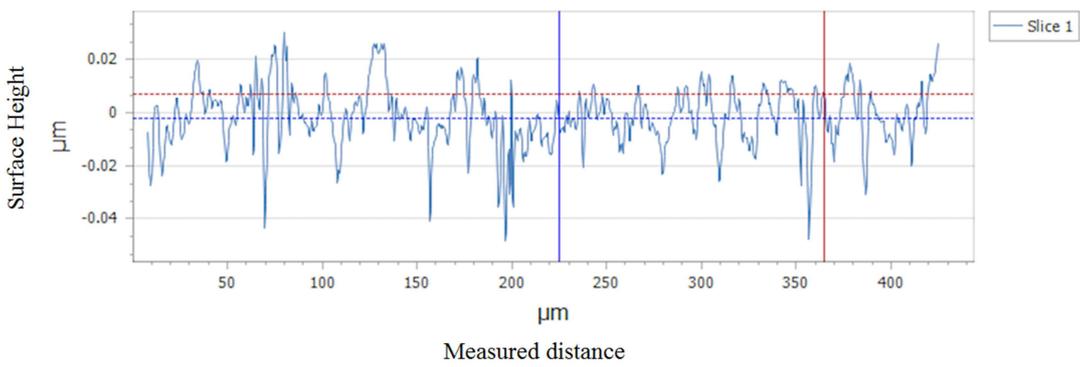
(b)

Figure 12. Surface Roughness Profile for the First Experiment a) Before Polishing and b) After 20 min. of Polishing.
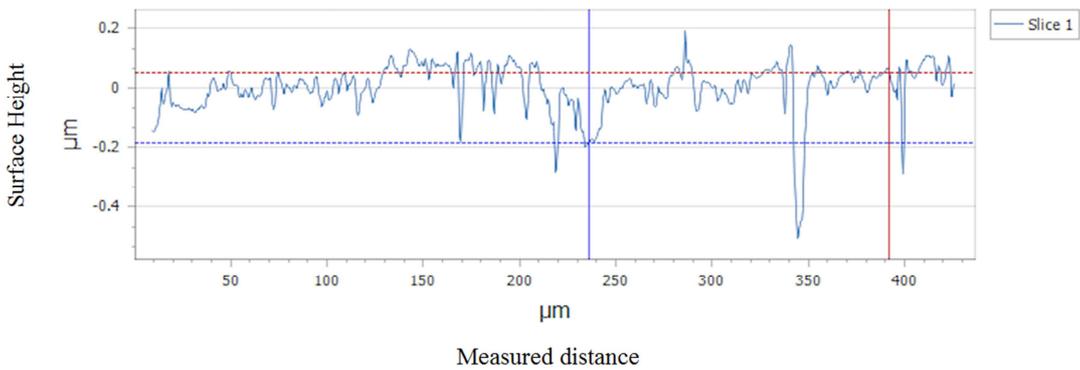
(a)
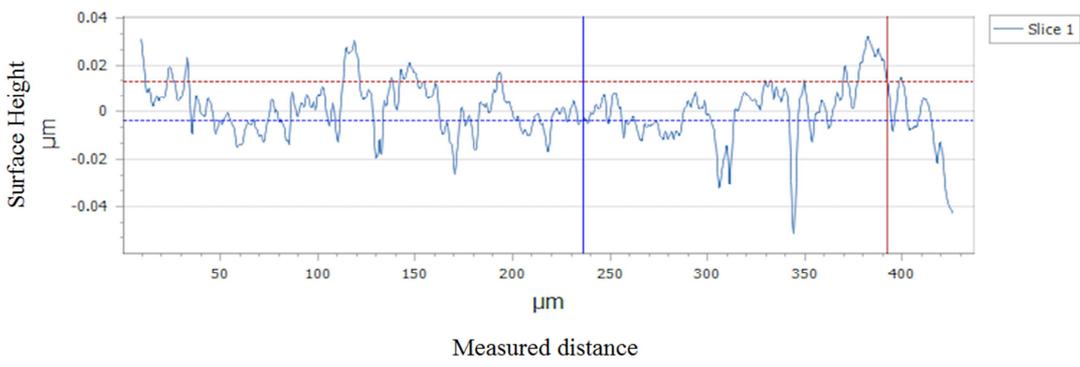
(b)

Figure 13. Surface Roughness Profile for the Second Experiment a) Before Polishing and b) after 30 min. of Polishing.

Table 2. *Surface Roughness Values Before and After Polishing for the two Experiments.*

Surface roughness parameter	Experiment 1		Experiment 2	
	Before polishing	After polishing	Before polishing	After polishing
S_a [μm]	0.097	0.012	0.053	0.008
S_q [μm]	0.128	0.017	0.081	0.011
S_z [μm]	1.410	0.642	2.930	0.534

6. Conclusion

The paper gives an investigation into the shape adaptive bonnet polishing. In this paper the tool imprints of shape adaptive bonnet polishing have been modelled to analyze the process. The experimental results show consistent results with the analytical model. Shape adaptive bonnet polishing proved its effectiveness in enhancing the workpiece surface roughness by ten times in addition to producing a smooth and uniform workpiece surface. The effects of polishing time and tool offset on the workpiece surface have been studied as well. The results proved that polishing time is more significant than tool offset due its effect in producing a tool influence curve of high radius of curvature.

References

[1] H. C. Schniepp *et al.*, "Functionalized single graphene sheets derived from splitting graphite oxide," *J. Phys. Chem. B*, vol. 110, no. 17, pp. 8535–8539, May 2006, doi: 10.1021/JP060936F/SUPPL_FILE/JP060936FSI20060316_022250. PDF.

[2] Z. Zhang, J. Yan, and T. Kuriyagawa, "Manufacturing technologies toward extreme precision," *Int. J. Extrem. Manuf.*, vol. 1, no. 2, p. 022001, Jun. 2019, doi: 10.1088/2631-7990/AB1FF1.

[3] C. Li, Y. Wu, X. Li, L. Ma, F. Zhang, and H. Huang, "Deformation characteristics and surface generation modelling of crack-free grinding of GGG single crystals," *J. Mater. Process. Technol.*, vol. 279, p. 116577, May 2020, doi: 10.1016/J. JMATPROTEC.2019.116577.

[4] M. J. Jackson, "Recent advances in ultraprecision abrasive machining processes," *SN Appl. Sci.*, vol. 2, no. 7, pp. 1–26, Jul. 2020, doi: 10.1007/S42452-020-2982-Y/FIGURES/19.

[5] X. Liu, X. Zhang, F. Fang, and Z. Zeng, "Performance-controllable manufacture of optical surfaces by ultra-precision machining," *Int. J. Adv. Manuf. Technol.*, vol. 94, no. 9–12, pp. 4289–4299, Feb. 2018, doi: 10.1007/S00170-017-1074-7/METRICS.

[6] M. J. Tsai and J. F. Huang, "Efficient automatic polishing process with a new compliant abrasive tool," *Int. J. Adv. Manuf. Technol.*, vol. 30, no. 9–10, pp. 817–827, Sep. 2006, doi: 10.1007/S00170-005-0126-6/METRICS.

[7] T. Kuriyagawa, M. Saeki, and K. Syoji, "Electrorheological fluid-assisted ultra-precision polishing for small three-dimensional parts," *Precis. Eng.*, vol. 26, no. 4, pp. 370–380, Oct. 2002, doi: 10.1016/S0141-6359(02) 00112-5.

[8] Y. Namba, N. Ohnishi, S. Yoshida, K. Harada, K. Yoshida, and T. Matsuo, "Ultra-Precision Float Polishing of Calcium Fluoride Single Crystals for Deep Ultra Violet Applications," *CIRP Ann.*, vol. 53, no. 1, pp. 459–462, Jan. 2004, doi: 10.1016/S0007-8506(07) 60739-2.

[9] M. J. Tsai, J. F. Huang, and W. L. Kao, "Robotic polishing of precision molds with uniform material removal control," *Int. J. Mach. Tools Manuf.*, vol. 49, no. 11, pp. 885–895, Sep. 2009, doi: 10.1016/J. IJMACHTOOLS.2009.05.002.

[10] C. J. Evans *et al.*, "Material Removal Mechanisms in Lapping and Polishing," *CIRP Ann.*, vol. 52, no. 2, pp. 611–633, Jan. 2003, doi: 10.1016/S0007-8506(07) 60207-8.

[11] W. Le Zhu and A. Beaucamp, "Compliant grinding and polishing: A review," *Int. J. Mach. Tools Manuf.*, vol. 158, p. 103634, Nov. 2020, doi: 10.1016/J. IJMACHTOOLS.2020.103634.

[12] Z. Wu, J. Shen, Y. Peng, and X. Wu, "Review on ultra-precision bonnet polishing technology," *Int. J. Adv. Manuf. Technol.*, vol. 121, no. 5–6, pp. 2901–2921, Jul. 2022, doi: 10.1007/S00170-022-09501-9/METRICS.

[13] M. Y. Chen, Y. T. Feng, Y. J. Wan, Y. Li, and B. Fan, "Neural network based surface shape modeling of stressed lap optical polishing," *Appl. Opt. Vol. 49, Issue 8, pp. 1350-1354*, vol. 49, no. 8, pp. 1350–1354, Mar. 2010, doi: 10.1364/AO.49.001350.

[14] H. Xu and K. Komvopoulos, "A quasi-static mechanics analysis of three-dimensional nanoscale surface polishing," *J. Manuf. Sci. Eng.*, vol. 132, no. 3, pp. 0309121–03091210, Jun. 2010, doi: 10.1115/1.4001582/434079.

[15] H. Xiao, Y. Dai, J. Duan, Y. Tian, and J. Li, "Material removal and surface evolution of single crystal silicon during ion beam polishing," *Appl. Surf. Sci.*, vol. 544, p. 148954, Apr. 2021, doi: 10.1016/J. APSUSC.2021.148954.

[16] X. Ke *et al.*, "Effect of the Binder during Ultra-Precision Polishing of Tungsten Carbide Using a Semirigid Bonnet Tool," *Mater. 2022, Vol. 15, Page 8327*, vol. 15, no. 23, p. 8327, Nov. 2022, doi: 10.3390/MA15238327.

[17] A. Beaucamp, Y. Namba, H. Combrinck, P. Charlton, and R. Freeman, "Shape adaptive grinding of CVD silicon carbide," *CIRP Ann.*, vol. 63, no. 1, pp. 317–320, Jan. 2014, doi: 10.1016/J. CIRP.2014.03.019.

[18] C. Wang *et al.*, "Highly efficient deterministic polishing using a semirigid bonnet," *https://doi.org/10.1117/1.OE.53.9.095102*, vol. 53, no. 9, p. 095102, Sep. 2014, doi: 10.1117/1. OE.53.9.095102.

[19] A. Beaucamp, Y. Namba, and P. Charlton, "Process mechanism in shape adaptive grinding (SAG)," *CIRP Ann.*, vol. 64, no. 1, pp. 305–308, Jan. 2015, doi: 10.1016/J. CIRP.2015.04.096.

[20] A. Beaucamp, P. Simon, P. Charlton, C. King, A. Matsubara, and K. Wegener, "Brittle-ductile transition in shape adaptive grinding (SAG) of SiC aspheric optics," *Int. J. Mach. Tools Manuf.*, vol. 115, pp. 29–37, Apr. 2017, doi: 10.1016/J. IJMACHTOOLS.2016.11.006.

[21] S. R. Bode, A. Kumar, and B. N. Singh, "Numerical analysis of single grit grinding on aluminum workpiece," *Vibroengineering Procedia*, vol. 29, pp. 291–294, Nov. 2019, doi: 10.21595/VP.2019.21150.

[22] A. Kareer, E. Tarleton, C. Hardie, S. V. Hainsworth, and A. J. Wilkinson, "Scratching the surface: Elastic rotations beneath nanoscratch and nanoindentation tests," *Acta Mater.*, vol. 200, pp. 116–126, Nov. 2020, doi: 10.1016/J. ACTAMAT.2020.08.051.

[23] A. S. Alaboodi and Z. Hussain, "Finite element modeling of nano-indentation technique to characterize thin film coatings," *J. King Saud Univ. - Eng. Sci.*, vol. 31, no. 1, pp. 61–69, Jan. 2017, doi: 10.1016/J. JKSUES.2017.02.001.

[24] Z. C. Cao, C. F. Cheung, and X. Zhao, "A theoretical and experimental investigation of material removal characteristics and surface generation in bonnet polishing," *Wear*, vol. 360–361, pp. 137–146, Aug. 2016, doi: 10.1016/J. WEAR.2016.03.025.

[25] K. Lee, K. P. Marimuthu, C. L. Kim, and H. Lee, "Scratch-tip-size effect and change of friction coefficient in nano / micro scratch tests using XFEM," *Tribol. Int.*, vol. 120, pp. 398–410, Apr. 2018, doi: 10.1016/J. TRIBOINT.2018.01.003.

[26] J. Zhang, H. Wang, A. Senthil Kumar, and M. Jin, "Experimental and theoretical study of internal finishing by a novel magnetically driven polishing tool," *Int. J. Mach. Tools Manuf.*, vol. 153, p. 103552, Jun. 2020, doi: 10.1016/J. IJMACHTOOLS.2020.103552.

[27] J. Zhang and H. Wang, "Generic model of time-variant tool influence function and dwell-time algorithm for deterministic polishing," *Int. J. Mech. Sci.*, vol. 211, p. 106795, Dec. 2021, doi: 10.1016/J. IJMECSCI.2021.106795.

[28] C. Wang *et al.*, "Modeling of the static tool influence function of bonnet polishing based on FEA," *Int. J. Adv. Manuf. Technol.*, vol. 74, no. 1–4, pp. 341–349, Jun. 2014, doi: 10.1007/S00170-014-6004-3/METRICS.

[29] X. L. Ke, C. J. Wang, Y. B. Guo, and Q. Xu, "Modeling of tool influence function for high-efficiency polishing," *Int. J. Adv. Manuf. Technol.*, vol. 84, no. 9–12, pp. 2479–2489, Jun. 2016, doi: 10.1007/S00170-015-7913-5/METRICS.